ELSEVIER

Journal of Organometallic Chemistry 568 (1998) 185–196

Journal of Organometallic Chemistry

Electrochemical study of methylfulvalene and methylcyclopentadiene molybdenum complexes

María-Luisa Marcos [a], Consuelo Moreno [b], Rosa M. Medina [b], María-José Macazaga [b], Salomé Delgado [b,*], Jaime González-Velasco [a]

[a] *Departamento de Química, Universidad Autónoma de Madrid, 28049 Madrid, Spain*
[b] *Departamento de Química Inorgánica, Universidad Autónoma de Madrid, 28049 Madrid, Spain*

Received 16 April 1998

Abstract

The product of the synthesis of (η^5:η^5-($C_5H_3Me)_2$)$Mo_2(CO)_6$ (**1**) is reported as a mixture of six stereoisomers, the ratio of which has been unambigously assigned using homonuclear two dimensional correlation spectroscopy (COSY and NOESY). The reaction of Li_2[(η^5:η^5-($C_5H_3Me)_2$)$Mo_2(CO)_6$] (**2**) with IMe yields (η^5:η^5-($C_5H_3Me)_2$)$Mo_2(CO)_6Me_2$ (**3**) and that of **1** with I_2 yields (η^5:η^5-($C_5H_3Me)_2$)$Mo_2(CO)_6I_2$ (**4**). The electrochemical behaviour of **1**, **3**, and **4** is reported and compared with analogous complexes where other substituents are present on the fulvalene rings. Electronic communication through the fulvalene ligand seems to take place in **4**. The related compounds [(η^5-C_5H_4R)$Mo(CO)_3]_2$ (R = Me (**5**), H (**9**)), (η^5-C_5H_4R)$Mo(CO)_3Me$ (R = Me (**7**), H (**10**)) and (η^5-C_5H_4R)$Mo(CO)_3I$ (R = Me (**8**), H (**11**)) have been synthesized in order to compare their electrochemical behaviour with the fulvalene analogous.

Keywords: Cyclopentadienyl; Molybdenum; Carbonyl complexes; Electrochemistry

---

1. Introduction

Bimetallic fulvalene (η^5:η^5-$C_{10}H_8$, Fv) complexes have centered the attention of different authors [1–6], due to their chemical behaviour, which may significantly differ from that shown by analogous cyclopentadienyl metal mononuclear and dimer complexes. One of the reasons for this difference may lie in the presence of the conjugated π-system of the fulvalene, which provides a mechanism for electronic communication between the metal centers regardless of whether or not there is a metal–metal bond, and whether the metal atoms are in *anti* or *syn* position with respect to the bridging ligand [7].

In spite of the comparatively few studies existing on related fulvalene and cyclopentadienyl complexes, spectroscopic evidence for electronic communication through the fulvalene ligand has been observed in the radical cations $FvFe_2(HMB)_2^+$ (HMB = hexamethylbenzene) [8] and $FvMn_2(CO)_4(\mu_2\text{-}PPh_2CH_2PPh_2)^+$ [9], and chemical evidence for this phenomenon has been provided by the conversion of the zwitterionic complexes $FvMo_2(CO)_5(PMe_3)_2$ and $FvMo_2(CO)_5$(dmpm) to $Mo(CO)_3(PMe_3)_3$ along with $FvMo(CO)_2(PMe_3)_2$ and $FvMo(CO)_2$(dmpm), respectively, in the presence of excess PMe_3 [10].

Of particular interest is the effect exerted by the presence of the fulvalene ligand in electron-transfer processes. In this sense, electrochemical evidence for electronic communication was found in the dirhodium system $FvRh_2(CO)_2(PPh_3)_2$, which undergoes a reversible, bielectronic oxidation at 0.01 V_{SCE}, whereas the cyclopentadienyl complex (η^5-C_5H_5)Rh(CO)(PPh_3) undergoes a monoelectronic oxidation at 0.43 V_{SCE}. This high difference in the oxidation potentials suggests

---

* Corresponding author. Fax: +34 91 3974833; e-mail: salome.delgado@uam.es

0022-328X/98/$19.00
PII S0022-328X(98)00722-0

that the formation of the cation in the first case is linked to a special stabilization which facilitates the oxidation process [11]. The presence of two distinct cathodic waves in the voltammetric reduction of $(\eta^5{:}\eta^5\text{-}(C_5H_3CO_2Me)_2)Mo_2(CO)_6I_2$ has been recently reported [12]. This behaviour contrasts with that found in the halocyclopentadienyl derivatives $(\eta^5\text{-}C_5H_5)M(CO)_3X$ (X = Cl, Br, I; M = Mo, W) [13,14] whose reduction gives rise to a single voltammetric wave, with a shape typical for an electroreduction process connected with an irreversible chemical process. This result is in agreement with the existence of electronic communication between the two metal centers via the fulvalene ligand.

The objective of this work is to extend the study to a series of closely related fulvalene and cyclopentadienyl complexes. Thus, we have performed the synthesis and the electrochemical study of the methyl-ring substituted fulvalene complex $(\eta^5{:}\eta^5\text{-}(C_5H_3Me)_2)Mo_2(CO)_6$ (**1**), its lithium salt $Li_2[(\eta^5{:}\eta^5\text{-}(C_5H_3Me)_2)Mo_2(CO)_6]$ (**2**) and the dimethyl $(\eta^5{:}\eta^5\text{-}(C_5H_3Me)_2)Mo_2(CO)_6Me_2$ (**3**) and diiodine $(\eta^5{:}\eta^5\text{-}(C_5H_3Me)_2)Mo_2(CO)_6I_2$ (**4**) derivatives together with the analogous methylcyclopentadienyl complexes $[(\eta^5\text{-}C_5H_4Me)Mo(CO)_3]_2$ (**5**), $Li[(\eta^5\text{-}C_5H_4Me)Mo(CO)_3]$ (**6**) and $(\eta^5\text{-}C_5H_4Me)Mo(CO)_3X$ (X = Me (**7**), I (**8**)) Scheme 1.

2. Experimental section

2.1. Reagents and general techniques

All manipulations were carried out by using standard Schlenk vacuum-line and syringe techniques under an atmosphere of oxygen-free Ar. All solvents for synthetic use were reagent grade. 1,2-Dimethoxyethane (DME), hexane and tetrahydrofurane (THF) were dried and distilled over sodium in the presence of benzophenone under an Ar atmosphere. Also under Ar, CH_2Cl_2 and acetone were dried and distilled over CaH_2 and $CaCl_2$, respectively. Propylene carbonate (PC) was stored over molecular sieves (5 Å) under Ar. All solvents were bubbled with Ar for 1 h after distillation and then stored under Ar, or degassed by means of at least three freeze-pump-thaw cycles after distillation and before use. Column chromatography was performed by using Alfa neutral alumina at activity II. Methyl iodide and $Li(Et)_3BH$ were used as received (Aldrich). The compounds $Na(DME)C_5H_4Me$ [15], $Mo(CO)_3(NCEt)_3$ [16], $[(\eta^5\text{-}C_5H_4Me)Mo(CO)_3]_2$ [17] (**5**), $[(\eta^5\text{-}C_5H_5)Mo(CO)_3]_2$ [17] (**9**), $(\eta^5\text{-}C_5H_5)Mo(CO)_3Me$ [18] (**10**) and $(\eta^5\text{-}C_5H_5)Mo(CO)_3I$ [19] (**11**) were prepared according to literature procedures. The dimethyldihydrofulvalene solution was prepared by a similar procedure used for the carbomethoxidihydrofulvalene [20].

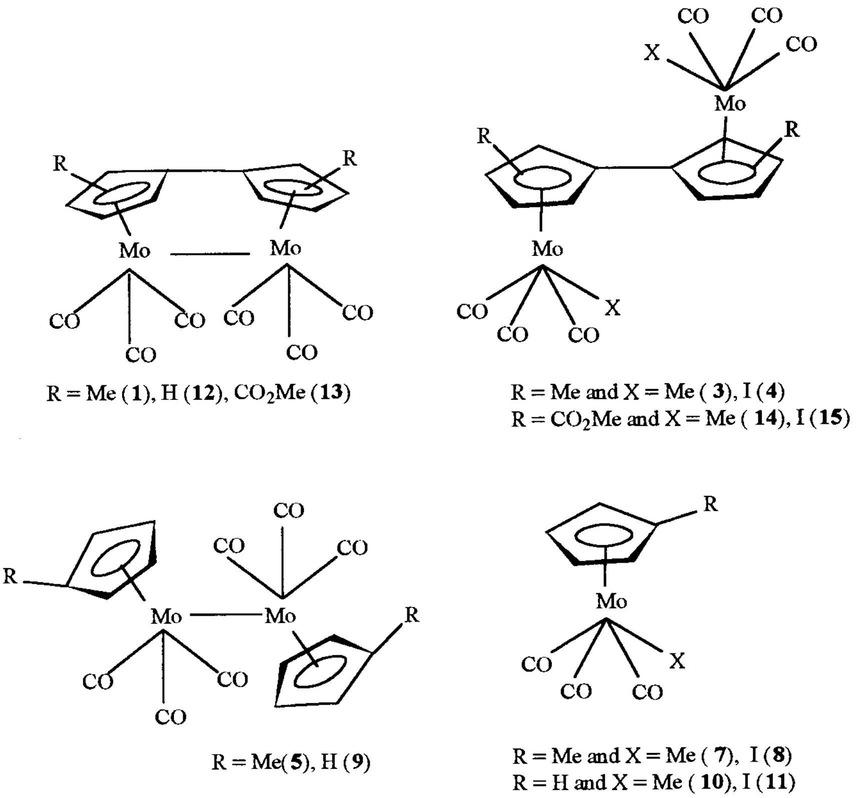

R = Me (**1**), H (**12**), CO_2Me (**13**)

R = Me and X = Me (**3**), I (**4**)
R = CO_2Me and X = Me (**14**), I (**15**)

R = Me(**5**), H (**9**)

R = Me and X = Me (**7**), I (**8**)
R = H and X = Me (**10**), I (**11**)

Scheme 1.

All reagents were used without further purification unless otherwise noted; **5, 9, 10** and **11** were purified by TLC. The ^{1}H-NMR spectra were recorded on a Bruker AMX-300 and 500 instrument. Chemical shifts were measured relative either to an internal reference of TMS or to residual protons of the solvents. IR spectra were measured on a Perkin-Elmer 1650 IR spectrometer. Elemental analyses were performed by the Mycroanalytical Laboratory of the University Autónoma of Madrid on a Perkin-Elmer 240 B microanalyser. Electronic spectra were recorded on a Pye Unicam SP 8-100 UV-visible spectrophotometer. Mass spectra were measured on a VG-Autospec mass spectrometer for FAB or AIE by the Mass Laboratory of the University Autónoma of Madrid.

2.2. Preparation of the isomer mixture of (η^5:η^5-($C_5H_3Me)_2$)$Mo_2(CO)_6$ (1)

A sample of $Mo(CO)_3(NCEt)_3$ (6.9 g, 20.0 mmol) in dry degassed glyme (400 ml) was heated to reflux under Ar. Without delay the dimethyldihydrofulvalene solution was added via syringe in 5-ml aliquots over a period of 4 h and the mixture refluxed for an additional 21 h. After being cooled, the entire reaction mixture was filtered through a CH_2Cl_2-packed alumina column (200 g). The column was washed with CH_2Cl_2 and the solution was concentrated to give a red powder; in the ^{1}H-NMR spectrum of this solid additional signals to those of the fulvalene ligand are observed. The solid was redissolved in CH_2Cl_2 and purified by thin-layer chromatography (TLC) using CH_2Cl_2/hexane (1:1) as eluent. Compound **1** was separated as a purple solid (0.9 g, 17%). [(η^5-C_5H_4Me)$Mo(CO)_3]_2$ and (η^5-C_5H_4Me)$Mo(CO)_3I$ were also obtained as red solids and were identified by IR and ^{1}H-NMR. **1**: ^{1}H-NMR (500 MHz, $CDCl_3$) δ 5.47 (t, 2H_{11}, $J_{11-12} = J_{11-13} = 2.2$ Hz); 5.34 (m, 1H_{21}, 1H_{31}); 5.32 (t, 1H_{41}, $J_{41-42} = \mathrm{J}_{41-43} = 2.2$ Hz); 5.26 (dd, 1H_{62}, $J_{62-61} = 1.8$ Hz, $J_{62-63} = 3.0$ Hz); 5.24 (dd, 1H_{52}, $J_{52-51} = 1.6$ Hz, $J_{52-53} = 3.0$ Hz); 5.22 (dd, 2H_{82}, $J_{82-81} = 1.8$ Hz, $J_{82-83} = 3.0$ Hz); 5.17 (dd, 2H_{71}, $J_{72-71} = 1.7$ Hz, $J_{72-73} = 3.0$ Hz); 5.02 (t, 1H_{22}, $J_{22-21} = J_{22-23} = 3.1$ Hz); 4.99 (t, 1H_{42}, $J_{42-41} = J_{42-43} = 3.1$ Hz); 4.95 (t, 1H_{32}, $J_{32-31} = J_{32-33} = 3.1$ Hz); 4.90 (t, 2H_{12}, $J_{12-11} = J_{12-13} = 3.0$ Hz); 4.44 (dd, 1H_{51}, $J_{51-52} = 1.6$ Hz, $J_{51-53} = 1.7$ Hz); 4.34 (dd, 1H_{63}, $J_{63-61} = 1.8$ Hz, $J_{63-62} = 3.1$ Hz); 4.25 (t, 1H_{61}, $J_{61-62} = J_{61-63} = 1.8$ Hz); 4.22 (t, 2H_{71}, $J_{71-72} = J_{71-73} = 1.7$ Hz); 4.17 (m, 2H_{13}, 2H_{81}); 4.09 (dd, 1H_{53}, $J_{53-51} = 1.7$ Hz, $J_{53-52} = 3.0$ Hz); 4.07 (dd, 2H_{83}, $J_{83-81} = 1.8$ Hz, $J_{83-82} = 3.0$ Hz); 4.02 (dd, 2H_{73}, $J_{73-71} = 1.7$ Hz, $J_{73-72} = 3.0$ Hz); 4.01 (dd, 2H_{23}, $J_{23-21} = 2.0$ Hz, $J_{23-22} = 3.1$ Hz); 3.95 (dd, 1H_{43}, $J_{43-41} = 1.8$ Hz, $J_{43-42} = 3.1$ Hz); 3.93 (dd, 1H_{33}, $J_{33-31} = 1.8$ Hz, $J_{33-32} = 3.1$ Hz); 2.19 (s, 3H_5, CH_3), 2.18 (s, 3H_6, CH_3), 2.16 (s, 6H_7, CH_3), 2.14 (s, 6H_8, CH_3), 1.83 (s, 6H_1, CH_3), 1.79 (s, 6H_2, CH_3), 1.63 (s, 3H_3, CH_3), 1.62 (s, 3H_4, CH_3). MS: *m*/*e* 517 (M^+). UV (THF) λ_{max} 545. Anal. Calc. for $C_{18}H_{12}O_6Mo_2$: C, 41.89; H, 2.34. Found: C, 41.78; H, 2.46.

2.3. Li_2[(η^5:η^5-($C_5H_3Me)_2$)$Mo_2(CO)_6$] (2)

A 1 M solution of $Li(Et_3)BH$ in THF (0.75 ml, 0.75 mmol) was added dropwise to a solution of **1** (0.15 g, 0.30 mmol) in THF (30 ml) at 0°C. The reaction was followed by IR spectroscopy. During the addition period the solution gradually changed from purple to yellow. Et_3B was removed under high vacuum along with the solvent and gave **2** as a yellow, air-sensitive residue. ^{1}H-NMR (300 MHz, acetone-d_6) δ 5.29 (m), 5.27 (m), 5.18 (m), 5.11 (m), 5.02 (m), 4.86 (m), 4.83 (m), 4.73 (m), 4.69 (m), 4.66 (m), 4.62 (m) (a total of 36H, Fv), 2.18 (s), 2.16 (s), 2.15 (s), 2.11 (s), 2.00 (s), 1.98 (s), 1.93 (s), 1.92 (s) (a total of 36H, Fv–CH_3).

2.4. (η^5:η^5-($C_5H_3Me)_2$)$Mo_2(CO)_6Me_2$ (3)

A solution of **2** prepared from **1** (0.15 g, 0.30 mmol) in THF (20 ml) at 0°C was treated with methyl iodide (39 µl, 0.60 mmol). The reaction was IR monitored. The solvent was removed under vacuum and the product was purified by TLC using acetone/hexane (1:2) as eluent. A yellow residue was obtained (0.13 g, 80%). ^{1}H-NMR (300 MHz, $CDCl_3$). δ 5.41 (m), 5.35 (m), 5.27 (m), 5.24 (m), 5.20 (m), 5.17 (m), 5.08 (m) (a total of 36H, Fv), 2.37 (s), 2.30 (s), 2.23 (s), 2.04 (s), 2.01 (s), 2.00 (s), 1.99 (s), 1.95 (s) (a total of 36H, Fv–CH_3), 0.28 (s), 0.25 (s), 0.24 (s), 0.23 (s), 0.22 (s) (a total of 36H, Mo–CH_3). UV (THF) λ_{max} 332 nm. Anal. Calc. for $C_{20}H_{18}O_6Mo_2$: C, 43.98; H, 3.32. Found: C, 43.86; H, 3.44.

2.5. (η^5:η^5-($C_5H_3Me)_2$)$Mo_2(CO)_6I_2$ (4)

Iodine (0.06 g, 0.24 mmol) in THF (20 ml) was added to a solution of **1** (0.12 g, 0.24 mmol) in THF (30 ml) with stirring. The color inmediately turned from purple to red. The solvent was removed under vacuum and the residue was purified by TLC using CH_2Cl_2/hexane (1:1) as eluent, giving **4** as the major product (0.15 g, 85%). ^{1}H-NMR (300 MHz, $CDCl_3$) δ 5.85 (m), 5.80 (m) 5.72 (m), 5.71 (m), 5.69 (m), 5.62 (m), 5.57 (m), 5.50 (m), 5.42 (m), 5.38 (m), 5.31 (m), 5.27 (m), 5.15 (m) (a total of 36H, Fv), 2.54 (s), 2.46 (s), 2.45 (s), 2.42 (s), 2.22 (s), 2.21 (s), 2.19 (s), 2.18 (s) (a total of 36H, Fv–CH_3). UV (THF) λ_{max} 490 nm. Anal. Calc. for $C_{18}H_{12}I_2O_6Mo_2$: C, 28.08; H, 1.57. Found: C, 27.95; H, 1.68.

2.6. Li[(η^5-C_5H_4Me)$Mo(CO)_3$] (6)

From a solution of **5** [17] (0.23 g, 0.44 mmol) in THF (20 ml) and 1 M solution of lithium triethylborohydride

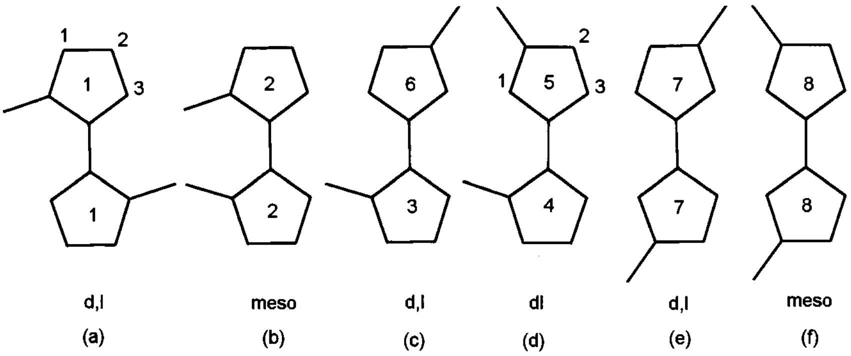

Fig. 1. Schematic representation of six possible isomers, not including enantiomers, of (η^5:η^5-($C_5H_3Me)_2)Mo_2(CO)_6$ (**1**).

in THF (1.1 ml, 1.1 mmol) and in the dark, a yellow air-sensitive oily-residue was obtained following the procedure described above for the preparation of **2**. ^{1}H-NMR (300 MHz, acetone-d$_6$) δ 4.89 (t, 2H, $J = 2.2$ Hz), 4.84 (t, 2H, $J = 2.2$ Hz), 1.97 (s, 3H).

2.7. (η^5-C_5H_4Me)$Mo(CO)_3Me$ (*7*)

From a solution of **6** (obtained from **5** [17] (0.23 g, 0.44 mmol) in THF (20 ml) and CH_3I (58 µl, 0.89 mmol) in the dark, a yellow oily-residue was obtained (0.20 g, 85%) following the procedure described above for the synthesis of **3** using hexane as eluent. ^{1}H-NMR (300 MHz, $CDCl_3$) δ 5.16 (t, 2H, $J = 2.2$ Hz), 5.11 (t, 2H, $J = 2.2$ Hz), 1.94 (s, 3H), 0.26 (s, 3H, Mo–CH_3). UV (THF) λ_{max} 313 nm. Anal. Calc. for $C_{10}H_{10}O_3Mo$: C, 43.82; H, 3.68. Found: C, 43.69; H, 3.80.

2.8. (η^5-C_5H_4Me)$Mo(CO)_3I$ (***8***)

The procedure described above for the preparation of **4** was used, but with **5** [17] (0.18 g, 0.35 mmol) and I_2 (0.088 g, 0.35 mmol) as reactants. The product was a red powder (0.23 g, 87%). ^{1}H-NMR (300 MHz, $CDCl_3$) δ 5.49 (t, 2H, $J = 2.2$ Hz), 5.38 (t, 2H, $J = 2.1$ Hz), 2.31 (s, 3H). MS: *m*/*e* 385 (M^+). UV (CH_2Cl_2) λ_{max} 484, 310 nm. Anal. Calc. for $C_9H_7IO_3Mo$: C, 28.01; H, 1.83. Found: C, 27.90; H, 1.94.

2.9. Electrochemical measurements

A computer-driven PAR Mo. 273 electrochemistry system with positive feedback IR compensation was employed. Measurements were carried out in a three electrode cell under N_2 atmosphere in anhydrous deoxygenated propylene carbonate (PC) containing 0.2 M tetrabutylammonium hexafluorophosphate ($TBAPF_6$) as supporting electrolyte. Temperature was maintained constant at 25°C. Cyclic voltammetry studies were made on a polycrystalline Pt working electrode (0.05 cm^2 real surface area, as calculated in a separate experiment through the H-adatom charge in 0.5 M H_2SO_4 solution [21]). The counterelectrode was a Pt gauze. The reference electrode was an Ag wire quasi-reference electrode (QRE), pre-treated by immersion in 10 M HNO_3 for 5 min before use. Ferrocene (Fc) was used as an internal standard, and all potentials in this paper were referred to the Fc^+/Fc couple, as IUPAC recommends [22]. When Fc caused wave overlapping, it was added to the solution immediately after a short series of experiments. Controlled potential coulometry studies were made on a large area Pt working electrode.

3. Results and discussion

3.1. Synthesis and spectroscopic properties

We have prepared a dimethyldihydrofulvalene solution by a similar procedure to that described by Delgado et al. [20] for the synthesis of a dicarbomethoxidihydrofulvalene solution. By reaction of this solution with $Mo(CO)_3(NCEt)_3$ complex **1** has been obtained as a mixture of six possible stereoisomers (Fig. 1). The reaction of **1** and $LiEt_3BH$ in THF at 0°C leads to the dianion salt **2**, which reacts with MeI to afford the dimethylated complex **3** in high yield. The diiodine complex **4** has been prepared from **1** and I_2 in THF.

The IR data of the complexes are listed in Table 1. The spectrum of **1** shows four absorption bands in the range 2100–1800 cm^{-1} associated with terminal Mo–CO stretching (ν_{CO}) modes, and the four bands observed in the spectrum of **2** are largely shifted to lower energies, due to a strong back donation from the metals to the CO ligands, as a consequence of the anionic nature of **2**. The dimethyl **3** and diiodine **4** derivatives show two IR terminal ν_{CO} bands, at 2010, 1926 cm^{-1} and 2033, 1962 cm^{-1}, respectively, which are indicative of C_s symmetry around each metal atom. The structures of **2**, **3** and **4** are expected to be similar to that of (η^5:η^5-($C_5H_3CO_2Me)_2)Mo_2(CO)_6I_2$ in which the fulvalene rings are planar [12]. In all these ring-dimethylated fulvalene complexes the ν_{CO} bands appear at lower frequencies than the corresponding band in the fulvalene [23] and dicarbomethoxyfulvalene [12,20] analogues. The trend observed in these ν_{CO} [24] is $CO_2MeFv > Fv > MeFv$ in accordance with an increase in the electronic density on the metal atom as the electron-donating capacity of the fulvalene ring substituent increases.

In the ^{1}H-NMR spectra of these complexes (mixture of six possible stereoisomers), eight separate methyl singlets are observed in the 2.5–1.6 ppm range, as expected if all different methyl signals were resolved. This mixture of isomers should exhibit 24 resonances due to fulvalene ring protons. In the spectrum of **1** 22 signals are observed in the 5.5–3.9 ppm range, however there is a considerable overlap of these resonances in the spectra of **3** and **4**, presumably due to a higher molecular symmetry as a consequence of the metal–metal bond rupture. We have assigned unambiguously the protons of the methyl groups and fulvalene rings of the six isomers of **1** by using homonuclear two-dimensional correlation spectroscopy (COSY, NOESY) [25] (Fig. 2). The ratio of d, l (**a**), meso (**b**), d, l (**c**), d, l (**d**), d, l (**e**), *meso* (**f**) was found to be 6:9:35:28:11:11 on the basis of integrals.

Similar reactions to those described above with the dimethylfulvalene complex (**1**) have been carried out with $[(\eta^5\text{-}C_5H_4Me)Mo(CO)_3]_2$ (**5**) in order to obtain the mononuclear complexes $Li[(\eta^5\text{-}C_5H_4Me)Mo(CO)_3]$ (**6**) and $(\eta^5\text{-}C_5H_4Me)Mo(CO)_3X$ (X = Me (**7**), I (**8**)). The IR spectrum of **6** shows four ν_{CO} bands (Table 1) at lower frequencies than those of **5** [26] as expected. The methyl **7** and iodine **8** derivatives show two terminal ν_{CO} bands at 2013, 1924, 2036 and 1952 cm^{-1}, respectively, in agreement with the cyclopentadienyl analogous compounds $(\eta^5\text{-}C_5H_5)Mo(CO)_3X$ (X = Me (**10**), I (**11**)) [18]. The ^{1}H-NMR spectra of **6**, **7** and **8** each display two triplet signals (A_2X_2 pattern) due to four cyclopentadienyl hydrogens and a singlet arising from the three protons of the cyclopentadienyl methyl group.

Table 1
IR spectroscopic data for the complexes **1**–**11** (cm^{-1}, THF)

No.	Compound	ν_{CO} (cm^{-1})
1	$(\eta^5\text{:}\eta^5\text{-}(C_5H_3Me)_2)Mo_2(CO)_6$	2012 (vs), 1955 (s), 1926 (vs), 1908 (s),1983 (w)
2	$Li_2[(\eta^5\text{:}\eta^5\text{-}(C_5H_3Me)_2)Mo_2(CO)_6]$	1890 (vs), 1802 (vs), 1775 (sh), 1712 (s)
3	$(\eta^5\text{:}\eta^5\text{-}(C_5H_3Me)_2)Mo_2(CO)_6Me_2$	2010 (s), 1926 (vs)
4	$(\eta^5\text{:}\eta^5\text{-}(C_5H_3Me)_2)Mo_2(CO)_6I_2$	2033 (vs), 1962 (vs)
5	$[(\eta^5\text{-}C_5H_4Me)Mo(CO)_3]_2$	2008 (m), 1952 (vs), 1909 (vs)
6	$Li[(\eta^5\text{-}C_5H_4Me)Mo(CO)_3]$	1902 (vs), 1804 (vs), 1778 (sh), 1716 (s)
7	$(\eta^5\text{-}C_5H_4Me)Mo(CO)_3Me$	2013 (s), 1924 (vs)
8	$(\eta^5\text{-}C_5H_4Me)Mo(CO)_3I$	2036 (vs), 1952 (vs)
9	$[(\eta^5\text{-}C_5H_5)Mo(CO)_3]_2$	2011 (m), 1954 (vs), 1911 (vs)
10	$(\eta^5\text{-}C_5H_5)Mo(CO)_3Me$	2016 (vs), 1926 (vs)
11	$(\eta^5\text{-}C_5H_5)Mo(CO)_3I$	2042 (vs), 1967 (vs)

3.2. Electrochemical studies

3.2.1. Electrochemistry of the fulvalene derivatives **1–4**

The voltammetric reduction of **1** in PC (Fig. 3) gives rise to a single cathodic peak. At 0.1 V s^{-1} the peak potential, E_{pc}, is -1.44 V versus Fc$^+$/Fc and the peak current function, i_{pc}/C, is 120 mA cm^{-2} M^{-1}. A reduced species is formed which can be reoxidized upon scan reversal at a much more positive potential, $E_{pa} = -0.54$ V. The reduction of **1** is bielectronic, as determined by controlled potential coulometry at -1.75 V. The function i_{pc} depends linearly on $v^{1/2}$ (v = scan rate) in the $0.01\ V\ s^{-1} < v < 1\ V\ s^{-1}$ range, whereas a plot of E_{pc} versus log v is linear for v up to 1 V s^{-1}. From the slope of this plot (50 mV decade^{-1}), the transfer coefficient αn_α corresponding to irreversible charge transfer can be calculated as 0.60 [27]. This value is consistent with that obtained from the peak width [27] ($E_{pc}-E_{pc/2} = 85$ mV), $\alpha n_\alpha = 0.56$.

The voltammetric behaviour is analogous to those of related compounds $FvMo_2(CO)_6$ [20,28] (**12**) and $(\eta^5\text{:}\eta^5\text{-}(C_5H_3CO_2Me)_2)Mo_2(CO)_6$ [20] (**13**). Thus, the reduction of **1** must also follow an ECE-type mechanism in which the first step is rate determining and consists of the addition of an electron that destabilizes the Mo–Mo bond. A relaxation of the molecule geometry through an increase in the Mo–Mo distance follows; this yields an anion radical easier to reduce than **1**, so that a second electron transfer readily takes place. The final product of the reduction process is the dianion $\mathbf{1}^{2-}$, in which there is no Mo–Mo bond. The identity of the final reduced species as $\mathbf{1}^{2-}$ is further confirmed by the voltammetric oxidation of $Li_2[(\eta^5\text{:}\eta^5\text{-}$

$(C_5H_4Me)_2)Mo_2(CO)_6]$, which contains the same anion and is oxidized in PC at -0.54 V ($v = 0.1$ V s^{-1}), the same E_{pa} found in the reoxidation of the reduction product of **1**.

The voltammetric oxidation of **1** (Fig. 4) originates an irreversible wave at $E_{ox} = +0.4$ V ($v = 0.1$ V s^{-1}) preceded by a prewave at ca. 0.2 V which disappears in the second and subsequent cycles for $v \geq 0.02$ V s^{-1}. The oxidation characteristics are analogous to those found for **12** [20,28] and **13** [20], and the process must correspond to the removal of electrons from orbitals that are primarily ligand-localized [20]. The prewave has been interpreted as being due to the formation of an adsorbed species on the electrode surface.

The influence of the substituents of the fulvalene rings on E_{pc} and E_{ox} is shown in Table 2. The E values obtained for a solution of **1** in PC have been compared with those for solutions of **12** and **13** in the same experimental conditions. E_{pc} shifts towards more negative potentials when the substituents (R) change from CO_2Me to H to CH_3. This result is in agreement with the electron-withdrawing or electron-donating properties of R. A similar trend is found for E_{ox}. Now, the CH_3 substituent makes the removal of electrons from **1** easier, i.e. E_{ox} is less positive. In the CO_2Me-substituted compound, where two isomers could be isolated [20] (**a** and **b**, see Fig. 1), E_{ox} was found to depend on the stereoisomer (0.65 and 0.56 V, respectively). In the

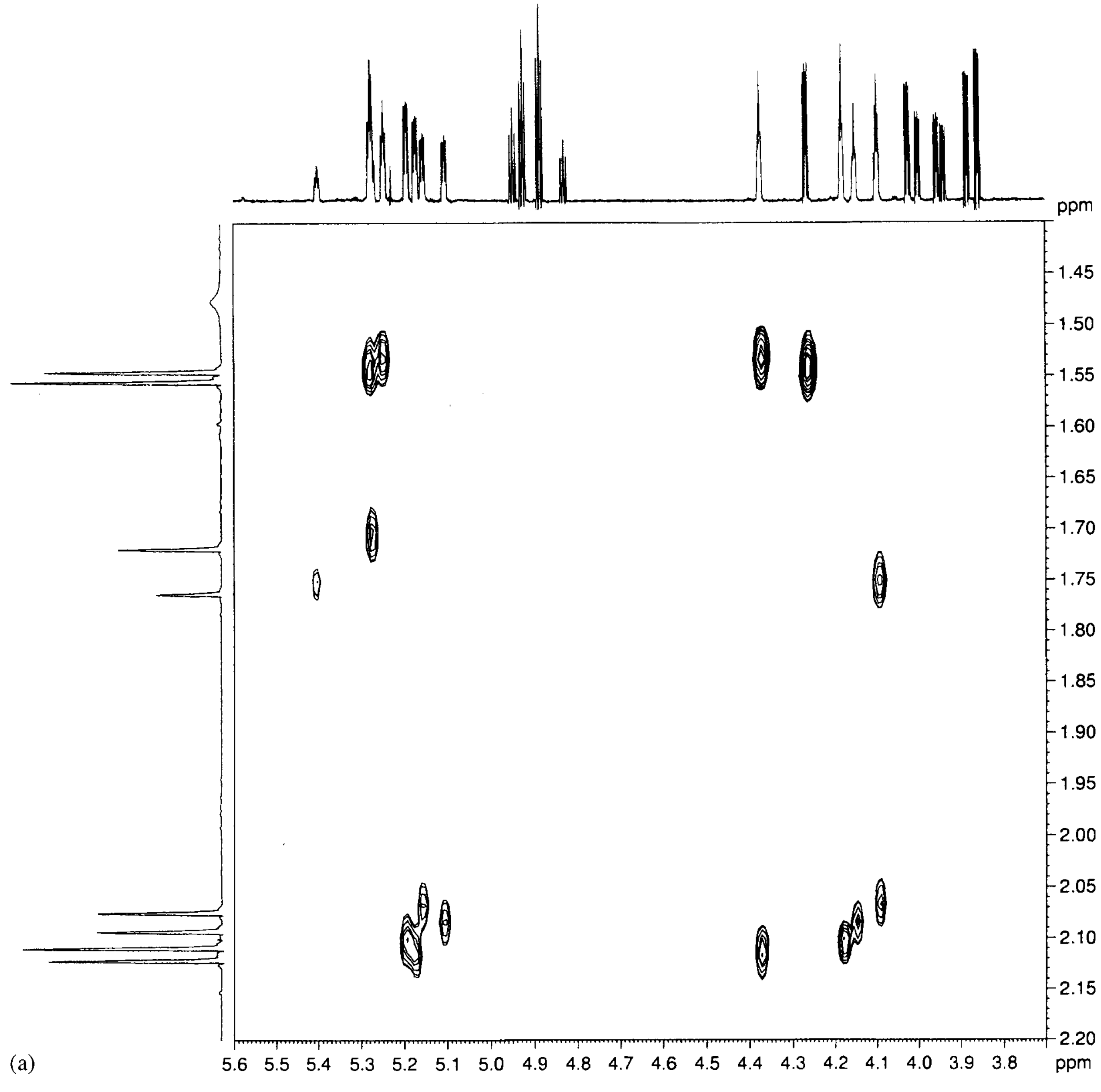

Fig. 2. NOESY experiment for $(\eta^5{:}\eta^5\text{-}(C_5H_3Me)_2)Mo_2(CO)_6$ (**1**) in $CDCl_3$.

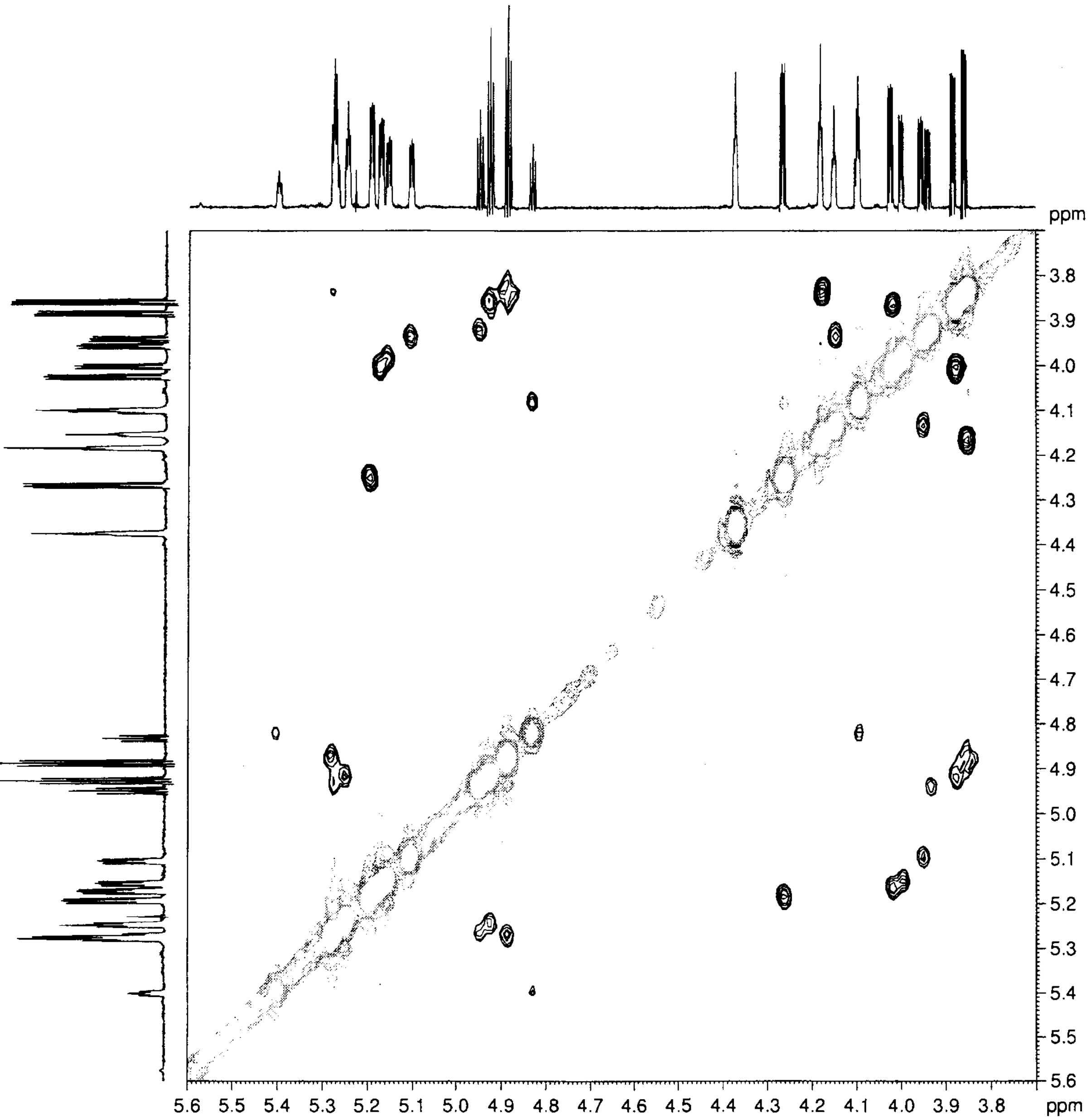

Fig. 2. (*Continued*)

same way, **1** is a mixture of six stereoisomers, and different E_{ox} should be expected. However, a single peak is observed in the voltammogram. This result must be due to the comparatively smaller shift in E_{ox} provoked by the presence of the CH_3 substituent in comparison with that found when $R = CO_2Me$ is the substituent. It is likely that each stereisomer in **1** originates a different E_{ox}, but the individual contributions cannot be resolved under the experimental conditions used, due to their close proximity.

Compounds **3, 4** do not contain a Mo–Mo bond, so that their electrochemical behaviour differs from that of **1**. The reduction of **3** originates as a single, poorly resolved, cathodic peak at ca. -2.25 V ($v = 0.1$ V s^{-1}) whilst that of **4** gives rise to two distinct cathodic waves (Fig. 5). The peak potentials, E_{pc1} and E_{pc2}, are -1.41 and -1.63 V at $v = 0.1$ V s^{-1}, respectively. Coulometry at -2.1 V shows that the overall reduction of **4** is a four-electron process, and the almost equal height of the two cathodic waves at low v ($i_{pc}/C = 140$ mA cm^{-2} M^{-1} at 0.1 V s^{-1}) indicates that each of them involves a two-electron transfer. $(\eta^5{:}\eta^5\text{-}(C_5H_3Me)_2)Mo_2(CO)_6^{2-}$ (**1**$^{2-}$) and I^- are the final products of the reduction of **4**. Upon scan reversal, **1**$^{2-}$ oxidizes to the Mo–Mo bonded compound **1** at -0.54 V, whilst I^- is oxidized at 0.08 V, as confirmed by the addition of an authentic sample of KI to the solution. When the anodic scan following the reduction of **4** is extended to ca. 1 V,

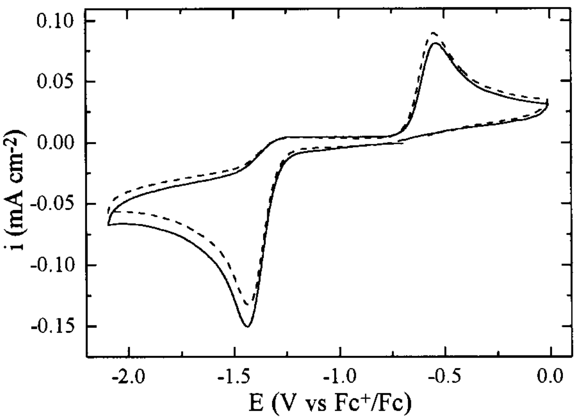

Fig. 3. Cyclic voltammogram for the reduction of a 1.26×10^{-3} M solution of **1** in PC containing 0.2 M $TBAPF_6$ at 0.1 V s^{-1} and 25°C. The first (—) and second (---) scans are shown.

additional peaks appear (Fig. 5). Two peaks at 0.63 and 0.86 V correspond to the oxidation of **4** and will be discussed later. A small peak at 0.4 V is also clearly distinguishable, and corresponds to the oxidation of **1**, which has been formed during the anodic sweep by the reoxidation of $\mathbf{1}^{2-}$ at -0.54 V. The two reduction waves of **4** are completely irreversible at low and moderate v. However, when $v \geq 2$ V s^{-1}, an oxidation peak coupled to the less cathodic wave can be observed (Fig. 6). The ratio i_{pa}:i_{pc} approaches 1 as v increases; at the same time, the intensity of the most cathodic reduction peak decreases relative to that of the less negative one.

The reduction behaviours of **3** and **4** are similar to those of $(\eta^5{:}\eta^5\text{-}(C_5H_3CO_2Me)_2)Mo_2(CO)_6(CH_3)_2$ (**14**) and $(\eta^5{:}\eta^5\text{-}(C_5H_3CO_2Me)_2)Mo_2(CO)_6I_2$ (**15**), respectively, whose electrochemical study in different solvents has been reported from this laboratory [12]. The reduction mechanisms of both species are still unclear, as the information gained from the mostly irreversible cyclic voltammograms is limited. Tetranuclear species such as reported by Astruc et al. [29] could be involved in the reduction process. The presence of two distinct cathodic waves in the case of **4** can be interpreted as due to electronic communication through the fulvalene ligand. If the two redox centers in **4** were completely non-interacting and independent of each other, a single cathodic wave would be expected, as each center would behave in a way similar to compound **8** (see below).

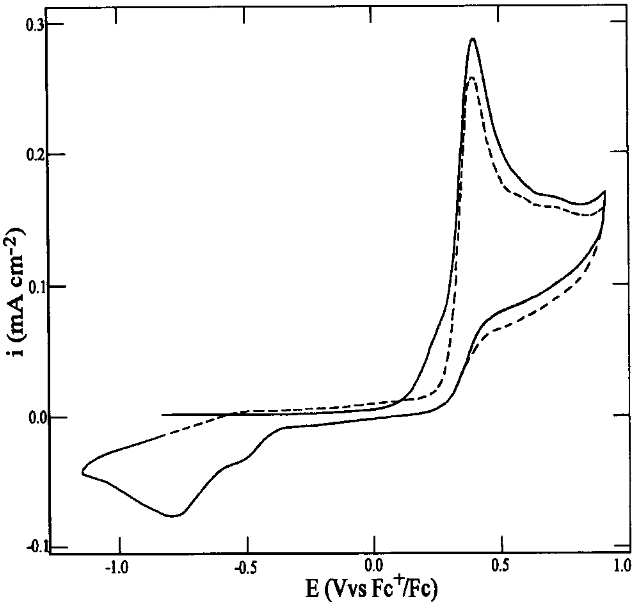

Fig. 4. Cyclic voltammogram for the oxidation of a 1.26×10^{-3} M solution of **1** in PC containing 0.2 M $TBAPF_6$ at 0.1 V s^{-1} and 25°C. The first (—) and second (---) scans are shown.

In the electrochemical oxidation of **4**, two irreversible peaks (Fig. 5, dashed line) are observed at $+0.63$ and $+0.86$ V ($v = 0.1$ V s^{-1}). No coupled cathodic peaks were recorded even at v as high as 80 V s^{-1}, which is in agreement with the existence of fast linked chemical reactions in solution. The peak current function i_{pc}/C of the first peak can be estimated as ca. 140 mA cm^{-2} M^{-1} at $v = 0.1$ V s^{-1}. At faster v the two anodic processes are best resolved, and the height of the second peak is about half that of the first one (Fig. 7).

The electrochemical oxidation of $(\eta^5{:}\eta^5\text{-}(C_5H_3CO_2Me)_2)Mo_2(CO)_6I_2$, **15** [12], leads to just one anodic peak when working in PC solution, whereas two peaks appeared when the solvent was acetonitrile. Several explanations can be postulated for the different behaviour of **4**: (a) an effect of the nature of the substituent, which not only influences the value of E_{ox}, but also is able to change the oxidation mechanism; (b) an effect of the position of the substituent. Complex **15** was prepared from an isolated isomer of **13** (**b**) in which both CO_2Me were on an α-C atom. On the contrary, **4** has been prepared from the isomer mixture **1**, and thus the substituents are both on α-C and β-C atoms. It is feasible that this may play a significant role in the oxidation of compound **4**. More work is in progress in order to ascertain the whole mechanism of the oxidation process.

A comparison of the peak potential data between **3** and its analogue **14**, and **4** and its analogue **15** is afforded in Table 2. The trend is similar to that found for the Mo–Mo bonded **1** and its analogues. Thus, both E_{pc} and E_{ox} shift towards more negative values when the electron-withdrawing CO_2Me substituents are replaced by the electron-donating CH_3. The amplitudes of the E_p shifts are very close to those found for the Mo–Mo bonded compounds.

3.3. Electrochemistry of the cyclopentadienyl dimer derivative **5**

The voltammetric reduction of $[(\eta^5\text{-}C_5H_4\text{-}Me)Mo(CO)_3]_2$, **5**, takes place through a single cathodic wave at $E_{pc} = -1.58$ V ($v = 0.1$ V s^{-1}). The reduced

Table 2
Peak potential values in PC at $v = 0.1$ Vs^{-1} for the reduction and oxidation processes

Compound	R	No.	E_{pc} (V vs. Fc^+/Fc)	E_{ox} (V vs. Fc^+/Fc)
$(\eta^5{:}\eta^5\text{-}(C_5H_3R)_2)Mo_2(CO)_6$	Me	**1**	−1.44	+0.40
	H	**12**	−1.40	+0.44
	CO_2Me	**13**	−1.20	+0.65[a]; +0.56[b]
$(\eta^5{:}\eta^5\text{-}(C_5H_3R)_2)Mo_2(CO)_6Me_2$	Me	**3**	−2.25	
	CO_2Me	**14**	−1.90	
$(\eta^5{:}\eta^5\text{-}(C_5H_3R)_2)Mo_2(CO)_6I_2$	Me	**4**	−1.41 and −1.63	+0.63 and +0.86
	CO_2Me	**15**	−1.20 and −1.50	+0.83
$[(\eta^5\text{-}C_5H_4R)Mo(CO)_3]_2$	Me	**5**	−1.58	+0.45
	H	**9**	−1.55	+0.52
$(\eta^5\text{-}C_5H_4R)Mo(CO)_3Me$	Me	**7**	−2.43	+0.50
	H	**10**	−2.36	+0.54
$(\eta^5\text{-}C_5H_4R)Mo(CO)_3I$	Me	**8**	−1.57	+0.63 and +0.95
	H	**11**	−1.51	+0.67 and +0.89

[a] Isomer **a**. [b] Isomer **b**.

species is reoxidized in a subsequent anodic scan at $E_{pa} = -0.55$ V (Fig. 8). The function i_{pc}/C (150 mA cm^{-2} M^{-1} at 0.1 V s^{-1}) linearly depends on $v^{1/2}$ in the 0.01 V s$^{-1} \leq v \leq 2$ V s^{-1} range. At the same time, E_{pc} shifts with v, and the plot of E_{pc} versus log v is linear for v up to 2 V s^{-1}. From the slope of this plot (80 mV decade^{-1}), the transfer coefficient αn_α can be calculated as 0.38. The reduction involves a bielectronic process, as indicated by controlled potential coulometry at −2.1 V. The reduced solution (yellow) could be reoxidized upon passage of ca. 2 F mol^{-1} to the original material **5** (red–orange).

The voltammetric behaviour of **5** resembles that of $[(\eta^5\text{-}C_5H_5)Mo(CO)_3]_2$, **9**, previously reported [30]. Thus, the bielectronic reduction of **5** must also proceed by a similar ECE-type mechanism ([30]b). A first rate determining electron transfer involves the weakening of the Mo–Mo bond and is followed by a fast homogeneous bond-breaking reaction yielding $[(\eta^5\text{-}C_5H_4Me)Mo(CO)_3]^-$ and $(\eta^5\text{-}C_5H_4Me)Mo(CO)_3$. The latter radical is easier to reduce than **5**, so that another electron is immediately added to this species, and a single bielectronic cathodic peak is observed. The mechanism is confirmed by the electrochemical behaviour of **6**, the lithium salt of $[(\eta^5\text{-}C_5H_4Me)Mo(CO)_3]^-$. In PC, **6** is oxidized at −0.55 V, i.e. the same value for E_{pa} found for the reoxidation of the reduction product of **5**. The reoxidation of $[(\eta^5\text{-}C_5H_4Me)Mo(CO)_3]^-$ yields **5** according to a well precedented EC path ([30]b) consisting in an electron transfer that yields the radical $(\eta^5\text{-}C_5H_4Me)Mo(CO)_3$ followed by dimerization to **5**.

The voltammetric oxidation of **5** gives rise to an irreversible peak at $E_{ox} = 0.45$ V ($i_{pc}/C = 340$ mA cm^{-2} M^{-1} at 0.1 V s^{-1}). This wave seems to be associated to a cathodic process at −0.9 V. For the related compound **9**, Kadish et al. ([30]b) suggested an ECE-type oxidation mechanism which, in the present case, would involve Eqs. (1–3):

$$[(\eta^5\text{-}C_5H_4Me)Mo(CO)_3]_2 \rightarrow [(\eta^5\text{-}C_5H_4Me)Mo(CO)_3]_2^+ + e^- \tag{1}$$

$$[(\eta^5\text{-}C_5H_4Me)Mo(CO)_3]_2^+ \rightarrow [(\eta^5\text{-}C_5H_4Me)Mo(CO)_3]^+ + (\eta^5\text{-}C_5H_4Me)Mo(CO)_3 \tag*{(‘2)}$$

$$(\eta^5\text{-}C_5H_4Me)Mo(CO)_3 \rightarrow [(\eta^5\text{-}C_5H_4Me)Mo(CO)_3]^+ + e^- \tag{3}$$

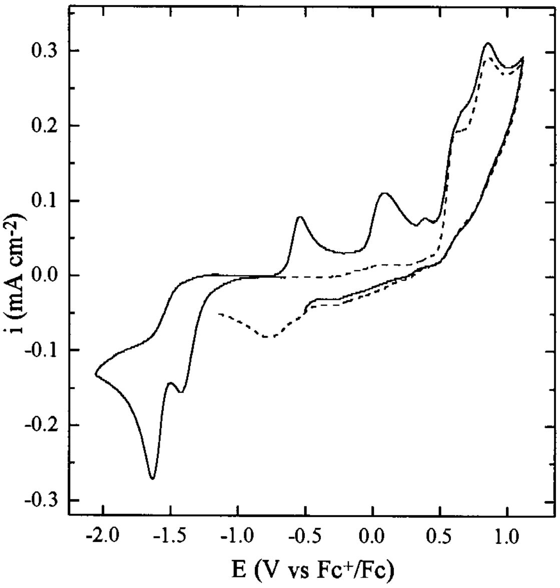

Fig. 5. Cyclic voltammograms of a 1.11×10^{-3} M solution of **4** in PC containing 0.2 M $TBAPF_6$ at 0.1 V s^{-1} and 25°C. Scans started at −0.6 V in the cathodic direction (—) and in the anodic direction (---).

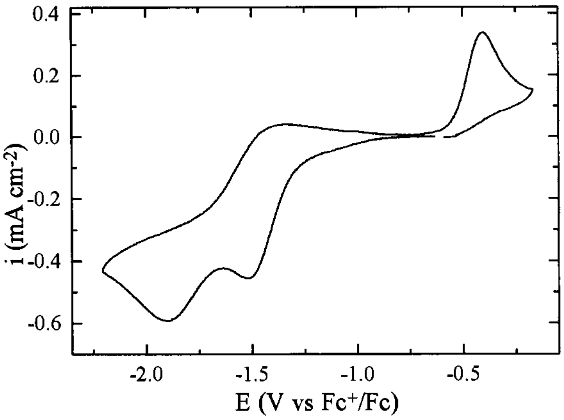

Fig. 6. Cyclic voltammogram for the reduction of a 7.3×10^{-4} M solution of **4** in PC containing 0.2 M $TBAPF_6$ at 2 V s^{-1} and 25°C. Scan started at -0.6 V in the cathodic direction.

Within the experimental conditions of this work, the first oxidation wave at 0.45 V is followed by a second and less intense one at 0.61 V which does not have a coupled reduction peak (Fig. 8). This latter peak could be due to a further oxidation of $[(\eta^5\text{-C}_5\text{H}_4\text{Me})\text{Mo(CO)}_3]^+$ or of another product resulting from a fast chemical reaction involving the monocation. A reduction wave at -0.71 V seems to be associated to this process. Kadish et al. ([30]b) did not report a second oxidation process for **9**, which can be due to the fact that they did not work in the same solvent. The oxidation of **9** in PC was also studied in the present work. It has been found that a first oxidation peak at 0.52 V, similar to that reported ([30]b), is followed by a second peak at 0.69 V. Table 2 assembles the values of E_{pc} and E_{ox} for **5** and **9** obtained under the same experimental conditions. They are more negative when the electron-donating substituent CH_3 is present, as expected. The amplitudes of the potential shifts are comparable to those found with **1** and **12**.

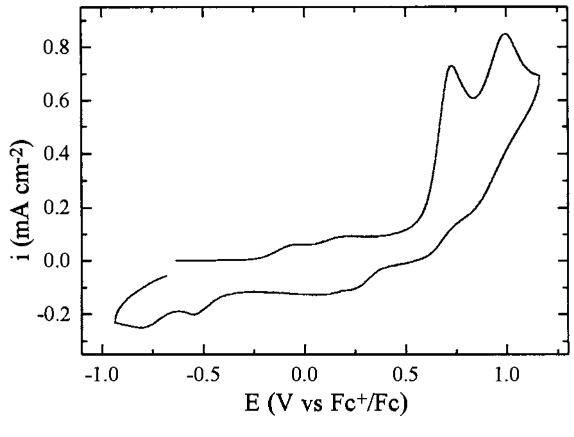

Fig. 7. Cyclic voltammogram for the oxidation of a 7.3×10^{-4} M solution of **4** in PC containing 0.2 M $TBAPF_6$ at 5 V s^{-1} and 25°C. Scan started at -0.6 V in the anodic direction.

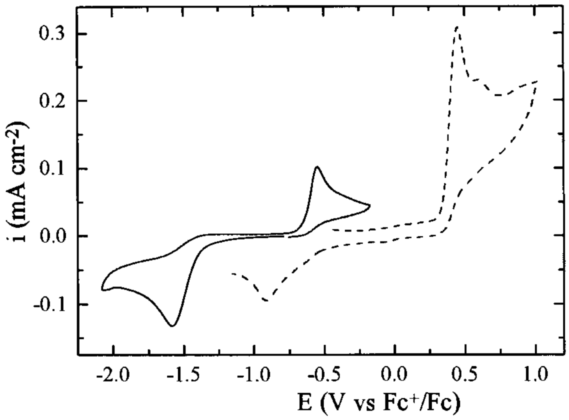

Fig. 8. Cyclic voltammograms of a 8.8×10^{-4} M solution of **5** in PC containing 0.2 M $TBAPF_6$ at 0.1 V s^{-1} and 25°C. Scans started at -0.8 V in the cathodic direction (—) and at -0.5 V in the anodic direction (---).

3.4. Electrochemistry of the cyclopentadienyl derivatives *7–8*

The reduction of $(\eta^5\text{-C}_5\text{H}_4\text{Me})\text{Mo(CO)}_3\text{Me}$, **7**, involves a cathodic wave at a very negative potential, $E_{pc} = -2.43$ V at $v = 0.1$ V s^{-1} (Fig. 9 and Fig. 10). The reduced species formed reoxidizes upon scan reversal at -0.55 V. A second cycle run immediately after the first one shows the appearance of a new cathodic peak at -1.58 V (0.1 V s^{-1}) which can be unambigously identified as due to the reduction of the dimer **5**. The voltammetric features and literature data [31] seem to indicate that the reduction of **7** takes place according to an EC scheme consisting in a first electron transfer followed by the breakage of the Mo–C bond

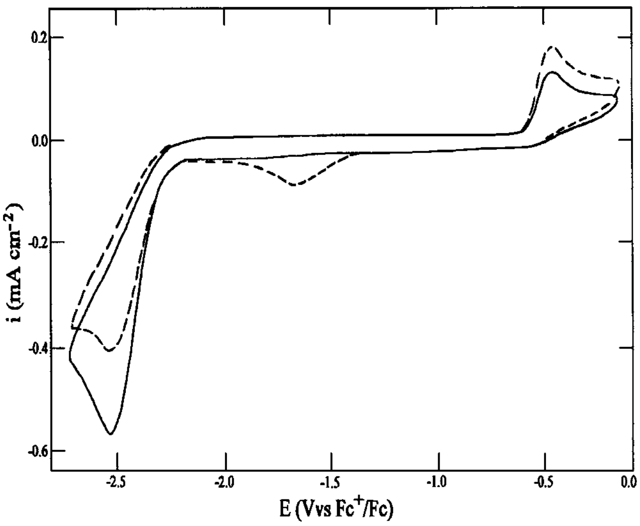

Fig. 9. Cyclic voltammogram of a 1.6×10^{-3} M solution of **7** in PC containing 0.2 M $TBAPF_6$ at 0.5 V s^{-1} and 25°C. The first (—) and the second (---) scans are shown. Scan started at -0.7 V in the cathodic direction.

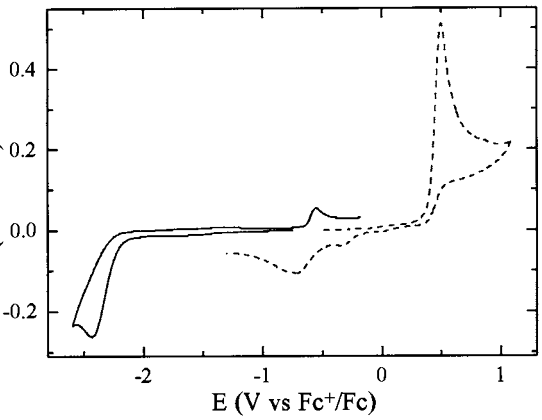

Fig. 10. Cyclic voltammograms of a 1.6×10^{-3} M solution of **7** in PC containing 0.2 M $TBAPF_6$ at 0.1 V s^{-1} and 25°C. Scans started at -0.7 V in the cathodic direction (—) and at -0.5 V in the anodic direction (---).

to yield $(\eta^5\text{-}C_5H_4Me)Mo(CO)_3^-$ and CH_3. The CH_3 radical evolves to CH_3CH_3 or CH_4 [31], whereas $(\eta^5\text{-}C_5H_4Me)Mo(CO)_3^-$ oxidizes upon scan reversal at -0.55 V, yielding **5**. This is confirmed by a reduction peak corresponding to **5** in the second cycle voltammogram.

The voltammetric oxidation of **7** gives rise to an irreversible wave with $E_{ox} = 0.50$ V (Fig. 10). The absence of a coupled cathodic peak indicates the existence of fast follow-up homogeneus chemical reactions. The current density measured seems to indicate a two-electron process, since the height of the oxidation peak is ca. twice that of the reduction peak, when adequate corrections for the baseline are made.

The electrochemical behaviour of **7** can be compared with that of $(\eta^5\text{-}C_5H_5)Mo(CO)_3Me$, **10**, which was prepared in order to obtain data in the same solvent. The voltammetric features of **10** in PC are similar to those of **7**, both for the reduction (irreversible monoelectronic wave at -2.36 V) and for the oxidation (irreversible two-electron wave at $+0.54$ V). In the reduction process, the anion $(\eta^5\text{-}C_5H_5)Mo(CO)_3^-$ is formed. This reoxidizes upon scan reversal to $(\eta^5\text{-}C_5H_5)Mo(CO)_3$, which readily dimerizes. The second cycle voltammogram shows then a reduction wave at -1.55 V corresponding to the dimer **9**. Values in Table 2 show that the effect of the CH_3 substituent is a negative shift of E_{pc} and E_{ox}. Interestingly, the amplitude of the shift in E_{pc} is larger than in **1**–**12** and **5**–**9**, where the reduction processes take place at primarily metal-localized orbitals, and concern the Mo–Mo bonds. On the other hand, the reduction of **7** and **10** is related to the Mo–C bond, and the energy of the orbitals where the electrons must enter seems to be more influenced by the substituents in the Cp ring.

The electrochemical behaviour of **8** was also investigated (Fig. 11). Reduction involves a single, completely irreversible, cathodic wave at $E_{pc} = -1.57$ V ($v = 0.1$ V s^{-1}, $i_{pc}/C = 148$ mA cm^{-2} M^{-1}). Coulometry indicates that the process is a two-electron transfer. Upon scan reversal, the reduction product is oxidized at -0.55 V (the same E_p as for the oxidation of **6**). The function i_{pc} depends linearly on $v^{1/2}$ in the $0.01\ V\ s^{-1} \leq v \leq 2\ V\ s^{-1}$ range. E_{pc} systematically shifts with v and, from the linear E_{pc} versus log v plot (slope = 80 mV decade^{-1}), $\alpha n_\alpha = 0.38$.

Complex **8** is closely related to $(\eta^5\text{-}C_5H_5)W(CO)_3X$ (X = Cl, Br, I), which were electrochemically studied under the same experimental conditions in this laboratory [14], and the voltammetric features of **8** are similar to those observed for the latter compounds. Thus, the bielectronic reduction of **8** must follow an ECE type mechanism analogous to that of Eqs. (3–5) in ref. [14], ie. electron transfer to **8**, Mo–I bond breaking to yield I^- and a $(\eta^5\text{-}C_5H_4Me)Mo(CO)_3$ radical, and final electron transfer to the latter. The product, $(\eta^5\text{-}C_5H_4Me)Mo(CO)_3^-$, is oxidized to **5** at -0.55 V upon scan reversal. A small anodic peak at 0.45 V is also clearly observed (Fig. 11), and can unambiguously be attributed to the oxidation of **5**. The peak at 0.07 V in Fig. 11 corresponds to the oxidation of I^-, as confirmed by the addition of an authentic sample of KI to the solution.

The oxidation of **8** takes place at $+0.63$ V ($v = 0.1$ V s^{-1}, $i_p/C = 102$ mA cm^{-2} M^{-1}). At low v, the anodic wave is completely irreversible (Fig. 11); however, at $v \geq 5$ V s^{-1} a coupled cathodic peak is observed, and i_{pc}/i_{pa} approaches one as v increases (Fig. 12). A second oxidation process, with no coupled cathodic wave even at $v = 80$ V s^{-1}, appears at $+0.95$ V at $v = 0.1$ V s^{-1}. The height of the first oxidation peak, and the reported results on related compounds [14,32] indicate that it involves one-electron transfer to yield $\mathbf{8}^+$. The latter suffers a follow-up chemical reaction which is not too

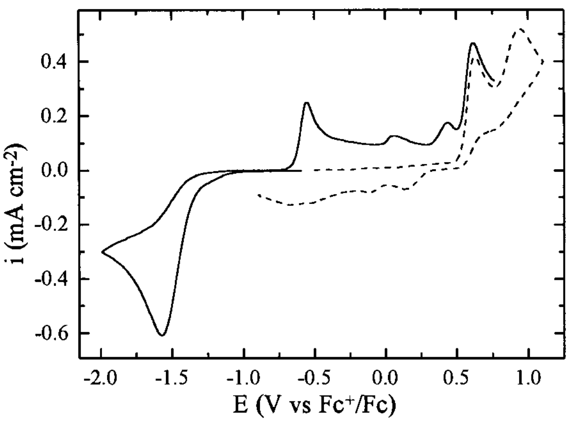

Fig. 11. Cyclic voltammograms of a 4.1×10^{-3} M solution of **8** in PC containing 0.2 M $TBAPF_6$ at 0.1 V s^{-1} and 25°C. Scans started at -0.6 V in the cathodic direction (—) and at -0.5 V in the anodic direction (---).

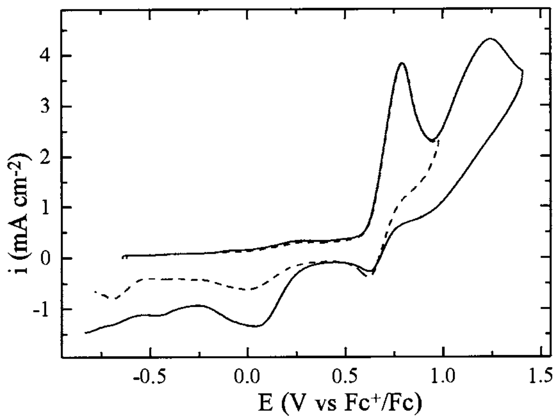

Fig. 12. Cyclic voltammograms of a 4.1×10^{-3} M solution of **8** in PC containing 0.2 M $TBAPF_6$ at 10 V s^{-1} and 25°C. Scans started at −0.7 V in the anodic direction.

fast in the time scale of the cyclic voltammetry experiment, as the presence of a coupled reduction peak for $v \geq 5$ V s^{-1} indicates. For the above mentioned (η^5-C_5H_5)$W(CO)_3X$ (X = Cl, Br, I) [14], the corresponding cations were too unstable to detect any sign of reversibility even at 80 V s^{-1}. However, when one of the CO ligands was replaced by the bulky PCy_3 (Cy = C_6H_{11}) in (η^5-C_5H_5)$W(CO)_2(PCy_3)I$, the 17-electron cationic species was greatly stabilized, and a coupled cathodic peak was observed at a scan rate as low as 0.02 V s^{-1}. For the related compounds (η^5-C_5H_5)$Mo(CO)_3X$ (X = Cl, Br, I), monoelectronic irreversible oxidation waves were found in acetonitrile, but the oxidation of the iodine compound was reversible at 5 V s^{-1} in DCM [32]. As the solvent seems to take a significant part in the stabilization of the cation, we have also prepared (η^5-C_5H_5)$Mo(CO)_3I$, **11**, and studied its electrochemical behaviour in PC. The voltammetric features of **11** are similar to those of **8**, as expected, but the presence of a coupled cathodic peak in the oxidation process cannot be detected until v is 10 V s^{-1} or faster. Thus, the CH_3 substituent in **8** involves a slight stabilization of the corresponding 17-electron $\mathbf{8}^+$ species as compared to $\mathbf{11}^+$, and this result can be attributed to the electron-donating character of CH_3. Table 2 shows the effect of the substituent on E_{pc} and E_{ox}. A trend towards more negative values is observed when R=H is replaced by R=CH_3.

Acknowledgements

We express our great appreciation of financial support from the DGICYT (Project PB 91-0003). Spain.

References

[1] J.S. Drage, K.P.C. Vollhardt, Organometallics 5 (1986) 280.
[2] P.A. McGovern, K.P.C. Vollhardt, Synlett (1990) 493.
[3] R. Boese, M.A. Huffman, K.P.C. Vollhardt, Angew. Chem. Int. Ed. Engl. 30 (1991) 1463.
[4] H.E. Amouri, Y. Besace, J. Vaisserman, G. Jaouen, M.J. McGlinchey, Organometallics 13 (1994) 4426.
[5] M. Herberhold, M. Biersack, T.E. Bitterwolf, A.L. Rheingold, Z. Naturforsch. B Chem. Sci. 48 (2) (1993) 161.
[6] (a) A.P. Kahn, R. Boese, J. Blümel, K.P.C. Vollhardt, J. Organomet. Chem. 472 (1994) 149. (b) M. Lacoste, M.H. Delville-Desbois, N. Ardoin, D. Astruc, Organometallics 16 (1997) 2343 and references therein.
[7] C.A. Coulson, A. Streitwieser Jr, M.D. Poole, J.I. Brauman, Dictionary of π-Electron Calculations, Pergamon, London, 1965.
[8] M.H. Desbois, D. Astruc, J. Guillin, J.P. Mariot, F. Varret, J. Am. Chem. Soc. 107 (1985) 5280.
[9] C.G. Atwood, W.E. Geiger, A.L. Rheingold, J. Am. Chem. Soc. 115 (1993) 5310.
[10] M. Tilset, K.P.C. Vollhardt, R. Boese, Organometallics 13 (1994) 3146.
[11] N.G. Connelly, A.R. Lucy, J.D. Payne, A.M.R. Galas, W.E. Geiger, J. Chem. Soc. Dalton Trans. (1983) 1879.
[12] C. Moreno, M.L. Marcos, M.J. Macazaga, R.M. Medina, D.H. Farrar, J. Gonzalez-Velasco, S. Delgado, Organometallics, in press.
[13] R.E. Dessy, R.B. King, M. Waldrop, J. Am. Chem. Soc. 88 (1966) 5112.
[14] M.L. Marcos, C. Moreno, M.J. Macazaga, et al., J. Organomet. Chem. 555 (1988) 57.
[15] J.C. Smart, C.J. Curtis, Inorg. Chem. 16 (1977) 1788.
[16] G.J. Kubas, Inorg. Chem. 22 (1983) 692.
[17] R. Birdwhistell, P. Hackett, A.R. Manning, J. Organomet. Chem. 157 (1978) 239.
[18] T.S. Piper, G. Wilkinson, J. Inorg. Nucl. Chem. 3 (1956) 104.
[19] E.W. Abel, A. Singh, G. Wilkinson, J. Chem. Soc. (1960) 1321.
[20] S. Delgado, M.J. Macazaga, R.M. Medina, et al., Organometallics 15 (1996) 5416.
[21] R. Woods, in: A.J. Bard (Ed.), Electroanalytical Chemistry, vol. 9, New York, 1976.
[22] (a) G. Gritzner, J. Kuta, Pure Appl. Chem. 54 (1982) 1527. (b) G. Gritzner, J. Kuta, Pure Appl. Chem. 56 (1984) 461.
[23] K.P.C. Vollhardt, T.W. Weidman, Organometallics 3 (1984) 82.
[24] ν_{co} data for $FvMo_2(CO)_6$ in THF: 2015.8, 1962.1, 1929.6, 1911.9, 1886.5 (our results).
[25] (a) H. Kessler, M. Gehrke, C. Griesinger, Angew. Chem. Int. Ed. Engl. 27 (1988) 490. (b) G.E. Martin, A.S. Zektler, Two-Dimensional NMR Methods for Establishing Molecular Connectivity, VCH, New York, 1988.
[26] R.D. Fischer, K. Noack, J. Organomet. Chem. 16 (1969) 125.
[27] R.S. Nicholson, I. Shain, Anal. Chem. 36 (1964) 706.
[28] R. Moulton, T.W. Weidman, K.P.C. Vollhardt, A.J. Baird, Inorg. Chem. 25 (1986) 1846.
[29] M.H. Delville-Desbois, D.S. Brown, K.P.C. Vollhardt, D. Astruc, J. Chem. Soc. Chem. Commun. (1991) 1355.
[30] (a) R.E. Dessy, F.E. Stary, R.B. King, M. Waldrop, J. Am. Chem. Soc. 88 (1966) 471. (b) K.M. Kadish, D.A. Lacombe, J.E. Anderson, Inorg. Chem. 25 (1986) 2246. (c) J.R. Pugh, T.J. Meyer, J. Am. Chem. Soc. 114 (1992) 3784.
[31] A. Chaloyard, N. El Murr, Inorg. Chem. 19 (1980) 3217.
[32] (a) Y. Lau, S. Gipson, Inorg. Chim. Acta 157 (1989) 147. (b) Y. Lau, W.W. Huckabee, S. Gipson, Inorg. Chim. Acta 41 (1990) 172.